Development of a soil-interface device for cyclic and large deformation shearing

Développement d'un appareil sol-interface pour cisaillements cycliques et larges déformations

Mir Amid Hashemi, Charles M. Heron

Nottingham Centre for Geomechanics, University of Nottingham, United Kingdom, Amid.Hashemi@nottingham.ac.uk

ABSTRACT: Challenges surrounding soil-structure interaction (SSI) problems motivate a significant amount of research in geotechnical engineering. Often, this SSI is cyclic in nature and can include large deformations such as in the case of pipelines or during pile driving. A new device has been developed at the University of Nottingham in order to study SSI through a series of tests involving large cyclic displacements of a structured material interface while the soil is subjected to vertical constant normal load or constant normal stiffness. A transparent soil container allows the particle-level soil movement and especially the shear band between the soil and the interface to be visualized and quantified through digital image correlation. The effect of confining pressure on the friction coefficient will be investigated as well as a correlation between the friction coefficient and the movement mode of soil particles in the shear band. The roughness of the interface before and after shearing and particle crushing through visualization will also be investigated.

RÉSUMÉ : Les défis autour des interactions de structures sol-interface (SSI) induit un grand nombre de recherches en ingénierie géotechnique. Souvent, ces interactions sont cycliques et peuvent inclure de larges déplacements comme dans le cas des pipelines. Un nouvel appareil a été développé à l'Université de Nottingham dans le but d'étudier les SSI via une série de tests impliquant de larges déplacements pendant que le sol est soumis ou bien à des charges verticales constantes ou bien à des rigidités constantes. Un récipient transparent permet de visualiser le mouvement du sol à l'échelle de la particule et plus particulièrement les bandes de cisaillement et une quantification peut être possible à l'aide de la vélocimétrie par images de particules. L'effet de la pression de confinement sur le coefficient de frottement et une corrélation entre le coefficient de frottement et le mode de mouvement des particules dans la bande de cisaillement seront étudiés. L'aspérité de l'interface et le broyage des particules avant et après le cisaillement seront également étudiés.

KEYWORDS: Soil-structure interaction, pipeline, particle crushing, image analysis.

1 INTRODUCTION

Characterisation of soil structure interface (SSI) behaviour is primordial to study of pipeline design. Oil and gas pipelines can experience cyclic displacements of varying amplitudes due to fluctuations in the fluid and soil temperatures. These axial displacements induce a shear friction between the surrounding soil and the pipelines outer surface. After a large number of cycles the coating might begin to wear and deteriorate even at low normal loads.

Previous studies have investigated the soil-structure interface through cyclic testing by the use of direct shear (Desai et al. 1985, Fioravante et al. 1999, Scarpelli et al. 2003, Ganesan et al. 2014), simple shear (Uesugi et al. 1989, Uesugi et al. 1990, Oumarou and Evgin 2005), 3D monotonic loadings (Fakharian and Evgin 1996) and pull-out tests (Alam et al. 2013, Martinez et al. 2015). Particle image velocimetry has more recently been used to analyse shear band developments (Dejong et al. 2006, DeJong and Westgate 2009). However, these studies have not been carried out for very large numbers of cycles (i.e. 1000-5000) or large displacements (i.e. 10mm) and therefore the effect of wearing and fatigue has not yet been studied. This paper describes the development of a large displacement shearing device and shows the first results from shearing tests between a coarse sand and a steel plate.

2 EXPERIMENTAL PROGRAM

2.1 *Experimental device*

Figure 1 shows a drawing of the experimental device. The soil sample is confined in a container which is fixed whereas the interface is attached to a shearing table that can move with a rail-carriage system. The horizontal and vertical actuations are made using a ball screw connected to a stepper motor, carrying out actuation at high precision. Both stepper motors are connected to controllers which are controlled by a computer.

The horizontal ball screw axis is located at the centre longitudinal axis of the device and goes through a clearance made in the shearing table. The horizontal load is measured by using two exchangeable load cells having a maximum load of 1kN each. These two load cells are attached to the shearing table and are located on each side of the horizontal ball screw. The horizontal displacement is measured by a large displacement LVDT sensor on the back of the device with a range of 310mm.

The vertical load cell is in-line with the vertical ball screw. It has a maximum load of 2.5kN. The vertical displacement is measured by a 10mm LVDT sensor attached under the vertical load cell. The soil sample is directly connected to the vertical LVDT and load cell via a top cap and is confined in a stainless steel circular container. This container can be replaced with a Perspex square shaped container to visualize grain scale deformations via particle image velocimetry (PIV).

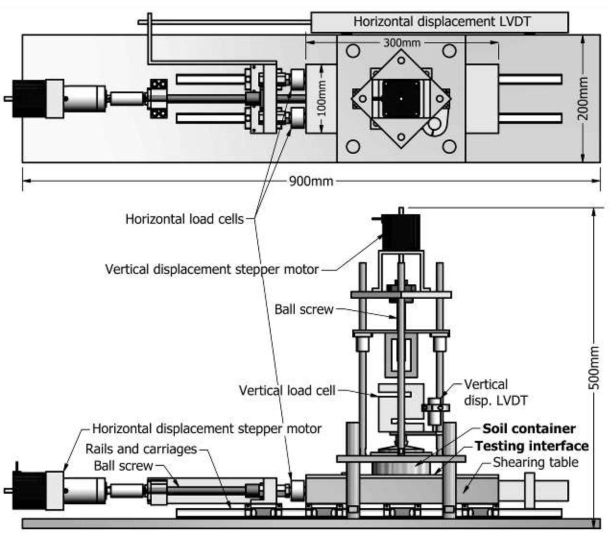

Figure 1. Detailed view of the soil-interface shearing device.

2.2 *Soil and interface properties*

The soil used in this experiment is a grade A coarse sand with a D_{50} = 1.66mm sieved from Leighton Buzzard sand. The grains are sub-angular and sub-rounded. Figure 2 shows its grain size distribution. The specific density is 2.65g/cm^3.

The interface is relatively a smooth stainless steel plate with a roughness R_t less than 1μm. Therefore the roughness factor R_n defined by (Uesugi, Kishida, and Tsubakihara 1989) as in Eq. 1 is less than 10^{-3}.

$$R_n = R_t/D_{50} \quad (1)$$

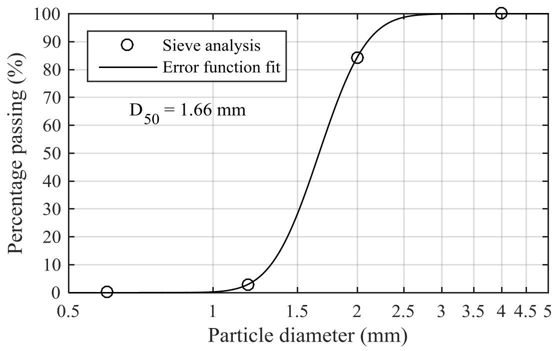

Figure 2. Grain size distribution of the Leighton Buzzard grade A sand.

3 EXPERIMENTAL PROCEDURE AND RESULTS

All soil samples were prepared by pouring the sand in the container. Their void ratio is equal to 0.64 and their relative density is equal to 90%. The soil-soil friction ratios are at 1.16 for peak and 0.8 for residual.

3.1 *Small displacement cycles (~1mm)*

Tests were carried out at three different constant normal loads: 250N, 500N and 1000N. These loads correspond to normal stresses of 65kPa, 130kPa and 260kPa respectively.

The first series of tests were carried out at a cyclic displacement of magnitude 1mm. Figure 3 shows a typical plot of the friction ratio as a function of horizontal displacement at different number of cycles. This test was carried out at a normal pressure of 260kPa.

The displacement rate is 0.5mm/s. It has been noticed that the rate of displacement does not change the cyclic behaviour significantly. Consequently, a relatively fast displacement rate has been chosen to shorten the time span of the cyclic tests. In the case of small displacement cycles, 5000 cycles correspond to a time span of 5hr 30mins.

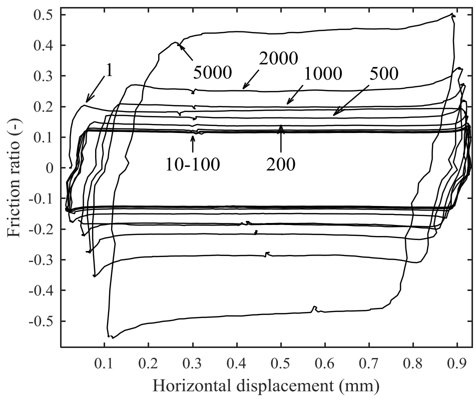

Figure 3. Example of a cyclic test showing friction ratio vs. horizontal displacement at different cycles.

In order to visualize more efficiently the change of friction ratio over time, an estimation of the mean friction ratio over an arbitrary distance can be calculated for each cycle. This arbitrary distance is taken where the friction ratio stays relatively constant. For example, for cyclic displacements of 1mm, the average is taken between 0.4mm and 0.6mm where it can be seen in Figure 3 that the friction ratio remains relatively constant. The mean friction ratio is shown in Figure 4 for the 65kPa vertical load as well as 130kPa and 260kPa.

It can be seen from Figure 4 that the friction ratio begins at 0.2 but rapidly decreases at 0.12 after a few cycles. Afterwards, the friction ratio increases back slowly after 30 cycles and goes up to 0.45 at 5000 cycles.

This trend can be seen in all three different normal loads (see Figure 4). Changing the normal load shows that no measurable change in friction ratio occurs below 100 cycles. However, beyond, the one having a normal load of 260kPa increases faster than the other two tests. Grain crushing also appeared for this last load in some locations. Grain crushing is identified through a sudden increase of shearing force, a sudden decrease of the sample height and a typical sound of crush during the shearing process.

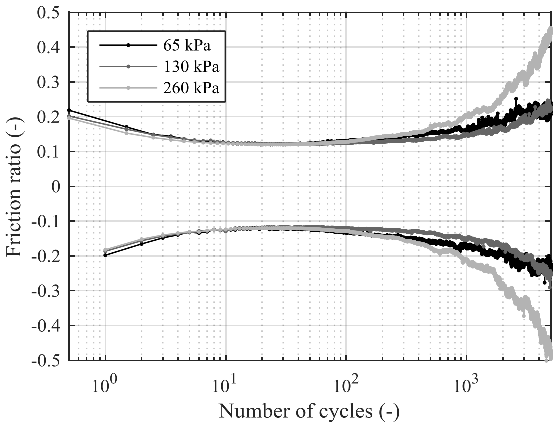

Figure 4. Mean friction ratio vs. number of cycles at different normal loads and at 1mm displacements.

3.2 *Large displacement cycles (~10mm)*

Larger cyclic tests have also been carried out at a displacement magnitude of 10mm at a displacement rate of 1mm/s. Every 180 cycles correspond to a time span of 1h.

At larger displacement cycles, particle breakage begins to appear. This feature was not observed at small displacement cycles except for a small degree in the 260kPa test. Figure 5 shows a long displacement cyclic test of 10mm with a normal load of 260kPa compared to the previous test shown in Figure 4 with a small displacement cycle and with the same normal load. Results show that particle breakage begins to appear after 200 cycles.

When different loads are compared together, it can be seen that particle breakage begins sooner for higher normal loads (see Figure 6): 200 cycles for 260kPa, 300 cycles for 130kPa and 700 cycles for 65kPa.

3.3 *Combination of small and large displacements*

In order to further understand the behaviour of grain crushing under cyclic loading, a test was performed with a combination of small displacement cycles (1500 cycles) followed by large displacement cycles until grain crushing. It can be seen (Figure 7) that grain crushing occurs at a fewer number of cycles than if a 10mm displacement was carried out from the beginning. Hence, cycle history is a critically important factor to consider.

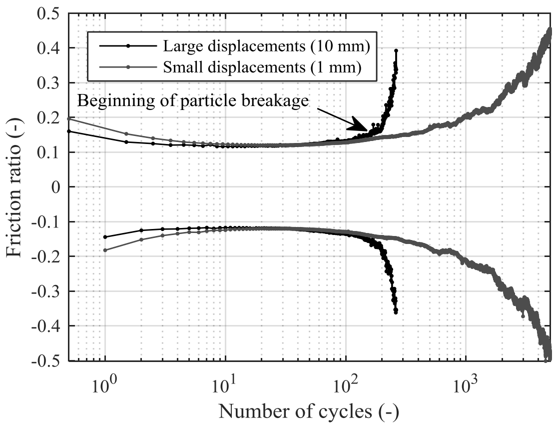

Figure 5. Comparison between large (~10mm) and small (~1mm) displacement cycles for the same vertical load of 260kPa.

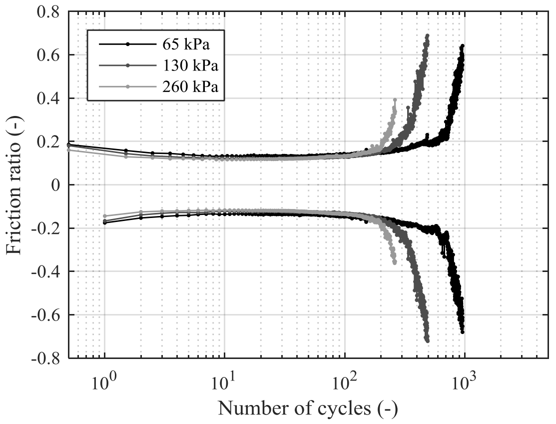

Figure 6. Particle breakage occurs sooner for higher normal loads with large displacement cycles.

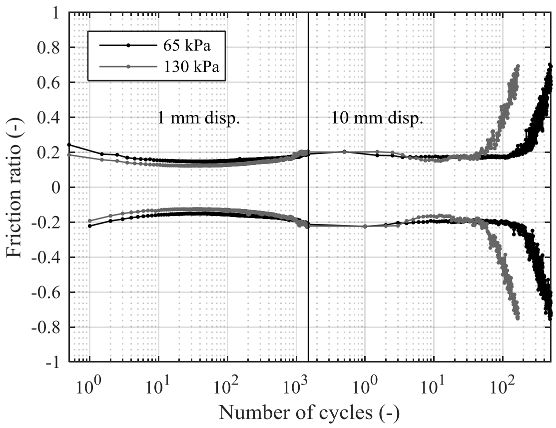

Figure 7. After 1500 cycles of 1mm, larger cycles of 10mm induce particle breakage sooner: 200 cycles for 65kPa load and 50 for 130kPa

3.4 *Surface damage of steel interface*

After soil-interface shearing, the damage of the steel plate surface can be investigated. In the Figure 8, the surface damage of four different tests are shown. Figure 8a to c are for tests at 1mm with vertical loads of 65kPa, 130kPa and 260kPa respectively.

Figure 8d is for a test at 10mm displacement under 260kPa load. a and b do not exhibit any grain crushing whereas c shows grain crushing in some locations. d exhibits grain crushing on all its surface. It can be seen that sand particles create straight grooves on the surface with a length corresponding to the displacement induced whereas grain crushing induces blurred zones with smeared damages.

3.5 *Perspex container for image analysis*

The shearing device can also be adapted with a square Perspex container. The container is a 50×50mm section and a camera is fixed on one side with LED lighting.

Images from a test are presented in Figure 9. Figure 9a is the initial configuration whereas Figure 9b is taken during shearing. A loosening of the structure is observed while particles on the interface crush and change the force chains in the upper layers of the sample. At the end (Figure 9c), crushed grains can be seen accumulating on the bottom while a settlement is observed as well.

4 DISCUSSIONS

4.1 *Decrease of friction ratio at low number of cycles*

The reason why friction ratio decreases in the beginning of all tests is believed to be due to the abrasion of sand particles on the steel surface. In the beginning of the tests, the sand particles have their own angularity. After a few cycles, this angularity decreases and adapts itself to the shape of the interface. On the other hand, the interface also adapts itself to the shape of the sand particles and grooves begin to form on the surface. Consequently, abrasion becomes less and less important as the contact surfaces between sand and steel increase. It should be noted that this abrasion of the sand particles is not considered ‘crushing’ in the context of this work.

4.2 Increase of friction ratio after 200 cycles

As shearing continues, the grooves on the interface become deeper and deeper. However, sand particles on the interface have reached their final abraded angularity. Consequently, a higher surface of contact induces a higher friction ratio. On the other hand, the asperity of the grooved part of the steel interface begins to increase as well because new zones of sand particles are abraded. At higher loads (such as 260kPa), grain crushing begins to appear after in some locations as can be seen in Figure 8c).

4.3 Particle breakage at large displacements

At the beginning of each test, the friction ratio is small. Therefore, all sand particles move together in a sliding manner. During each travel, all sand particles stay in their position. When the direction changes, only small rotation changes occur on the interface without changing the arrangement of the group.

However, when the friction ratio increases, the sand particles touching the interface begin to rotate continually (not just at change of direction). In the case of a displacement amplitude of 1mm, sand particles will not rotate sufficiently to affect their neighbours. But 10mm displacements will cause sand particles to make multiple full rotations. This will cause a disturbance in the region of the interface and particle breakage begins to occur. Once one particle breaks, it causes a rearrangement of force chains in the sample and provokes other sand particles to break as well in a snowball effect.

When two stage shearing is carried out (i.e. first 1mm then 10mm displacements), grain crushing appears much sooner in the second stage because the surface asperity exhibits already 1mm grooves. This will cause the particles to disturb more easily.

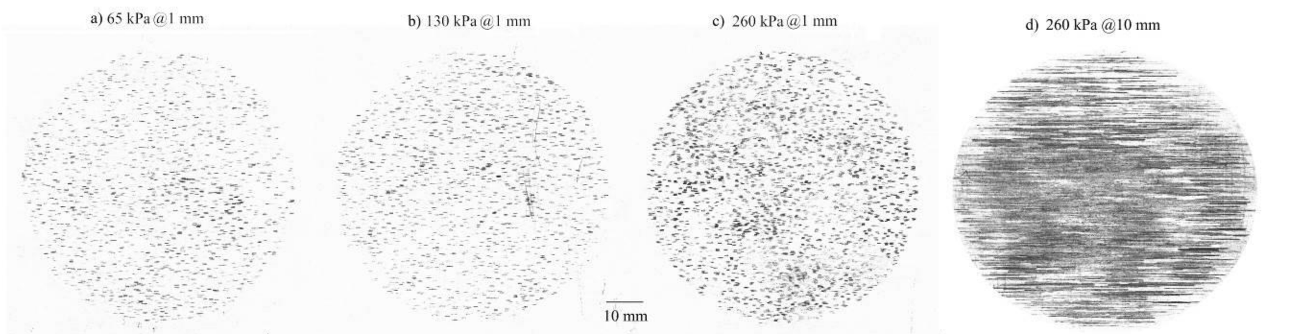

Figure 8. Damage of the plates after shearing. a) to c) are tests made with 1mm displacement and d) is with 10mm displacement. In c) grain crushing is visible in some locations. In d), grain crushing happened on all the surface.

Figure 9. Image analysis with a Perspex container. a) initial configuration. b) during middle term cyclic shearing. c) End of cyclic test.

5 CONCLUSIONS

This paper shows the preliminary results of a new device developed in the University of Nottingham for soil-interface shearing. This device allows the carrying out of cyclic large displacements up to 200mm. The soil container of this device can be adapted to receive a Perspex container where grain scale displacements can be investigated during shearing.

The first results show that cyclic shearing of sand on a stainless steel plate creates grooves on the surface and the friction ratio of the steel interface increases after approximately 200. This will inevitably cause a surface degradation of the plate which in turn will increase furthermore the friction ratio. After a given period, grains will begin to crush and lead to the friction ratio increasing at an ever higher rate.

This research is particularly interesting for the study of interface degradation on pipeline coatings where it is until now still not well understood how the degradation mechanism occurs and how this affects the long-term interaction behaviour.

This study has already highlighted that interface degradation depends on the normal load applied but, more importantly, on the displacement magnitude of the cyclic shearing. A higher displacement will induce sand grains to mobilize more provoking a destabilization at the interface. This will cause a higher probability of grain crushing. For the same accumulated displacement, tests with a larger displacement cause grain crushing sooner. It should be considered in design therefore that both cycle displacement history and cyclic amplitude will affect long term behaviour as demonstrated by the fact that grain crushing occurs sooner with larger amplitude cycles despite having accumulated less total shear displacement.

6 ACKNOWLEDGEMENTS

The Dean of Engineering Prize of the University of Nottingham is gratefully acknowledged for the development of this research.

7 REFERENCES

Alam S., Allouche E., Bartlett C., Sherpa A. and Keil B. 2013. Experimental evaluation of soil-pipe friction coefficients for coated steel pipes. In *Pipelines 2013*, 360-371. American Society of Civil Engineers.

DeJong J.T. and Westgate Z.J. 2009. Role of initial state, material properties, and confinement condition on local and global soil-structure interface behavior. *Journal of Geotechnical and Geoenvironmental Engineering* 135 (11), 1646-1660. doi: doi:10.1061/(ASCE)1090-0241(2009)135:11(1646).

Dejong J.T., White D.J. and Randolph M.F. 2006. Microscale observation and modeling of soil-structure interface behavior using particle image velocimetry. *Soils and Foundations* 46 (1), 15-28. doi: 10.3208/sandf.46.15.

Desai C.S., Drumm E.C. and Zaman M.M. 1985. Cyclic testing and modeling of interfaces. *Journal of Geotechnical Engineering* 111 (6), 793-815. doi: 10.1061/(ASCE)0733-9410(1985)111:6(793).

Fakharian K. and Evgin E. 1996. An automated apparatus for three-dimensional monotonic and cyclic testing of interfaces.

Fioravante V., Ghionna V.N., Pedroni S. and Porcino D. 1999. A constant normal stiffness direct shear box for soil-solid interface tests. *Rivista Italiana di Geotecnica* 33 (3), 7-22.

Ganesan S., Kuo M. and Bolton M. 2014. Influences on pipeline interface friction measured in direct shear tests.

Martinez A., Frost J. and Hebeler G. 2015. Experimental study of shear zones formed at sand/steel interfaces in axial and torsional axisymmetric tests.

Oumarou T.A. and Evgin E. 2005. Cyclic behaviour of a sand – steel plate interface. *Canadian Geotechnical Journal* 42 (6), 1695-1704. doi: 10.1139/t05-083.

Scarpelli G., Sakellariadi E. and Furlani G. 2003. Evaluation of soil-pipeline longitudinal interaction forces. *Rivista Italiana di Geotecnica* 4 (3), 24-41.

Uesugi M., Kishida H. and Tsubakihara Y. 1989. Friction between sand and steel under repeated loading. *Soils and Foundations* 29 (3), 127-137. doi: 10.3208/sandf1972.29.3_127.

Uesugi M., Kishida H. and Uchikawa Y. 1990. Friction between dry sand and concrete under monotonic and repeated loading. *Soils and Foundations* 30 (1), 115-128. doi: 10.3208/sandf1972.30.115.